ASTERICS - H2020 - 653477

Time transfer in SURFnet/LOFAR network & general design rules for network implementation

ASTERICS GA DELIVERABLE: D5.7

Document identifier:	
Date:	**21-09-2018**
Work Package:	**WP5**
Lead Partner:	**OPNT B.V.**
Document Status:	**Final**
Dissemination level:	**Public**
Document Link:	www.asterics2020.eu/documents/ASTERICS-D5.7.pdf

Abstract

This document describes the implementation of time and frequency transfer over up to 169 km of fiber using bi-directional White Rabbit links, in the already operational optical DWDM fiber network of SURFnet. Time and frequency stability and accuracy measurements indicate that this TFT method is suited for VLBI measurements.

I. COPYRIGHT NOTICE

II. DELIVERY SLIP

	Name	Partner	Date
From	J.C.J. Koelemeij	OPNT - **WP5**	21/09/2018
Author(s)	C. van Tour, R. Smets, P. Boven, P. Maat , J.C.J. Koelemeij, A. Szomoru	OPNT (van Tour and Koelemeij), SURFnet (Smets), JIVE (Boven and Szomoru), LOFAR (Maat) - **WP5**	21/09/2018
Reviewed by	Giuseppe Cimo`	WP1	15/09/2018
Approved by	AMST		

III. DOCUMENT LOG

Issue	Date	Comment	Author/Partner
0.3	12-09-2018	First draft	Chantal van Tour/OPNT
0.4	12-09-2018	Expanded uncertainty analysis	Paul Boven/JIVE
0.5	17-09-2018	Accepted Paul's changes + made some minor changes	Chantal van Tour/OPNT
0.6	19-09-2018	Added chapter 3	Rob Smets / SURFnet
0.7	20-09-2018	Added VLBI requirements and evaluation	Paul Boven / JIVE
0.8	20-09-2018	Combined input from R. Smets and P. Boven. Wrote abstract and executive summary	Chantal van Tour/OPNT
0.9	20-09-2018	Minor corrections	Paul Boven/JIVE

IV. APPLICATON AREA

This document is a formal deliverable for the GA of the project, applicable to all members of the ASTERICS project, beneficiaries and third parties, as well as its collaborating projects.

V. TERMINOLOGY

A complete project glossary is provided at the following page: http://www.asterics2020.eu/about/glossary/

VI. PROJECT SUMMARY

ASTERICS (Astronomy ESFRI & Research Infrastructure Cluster) aims to address the cross-cutting synergies and common challenges shared by the various Astronomy ESFRI facilities (SKA, CTA, KM3Net & E-ELT). It brings together for the first time, the astronomy, astrophysics and particle astrophysics communities, in addition to other related research infrastructures. The major objectives of ASTERICS are to support and accelerate the implementation of the ESFRI telescopes, to enhance their performance beyond the current state-of-the-art, and to see them interoperate as an integrated, multi-wavelength and multi-messenger facility.

An important focal point is the management, processing and scientific exploitation of the huge datasets the ESFRI facilities will generate. ASTERICS will seek solutions to these problems outside of the traditional channels by directly engaging and collaborating with industry and specialized SMEs. The various ESFRI pathfinders and precursors will present the perfect proving ground for new methodologies and prototype systems. In addition, ASTERICS will enable astronomers from across the member states to have broad access to the reduced data products of the ESFRI telescopes via a seamless interface to the Virtual Observatory framework. This will massively increase the scientific impact of the telescopes, and greatly encourage use (and re-use) of the data in new and novel ways, typically not foreseen in the original proposals.

By demonstrating cross-facility synchronicity, and by harmonizing various policy aspects, ASTERICS will realize a distributed and interoperable approach that ushers in a new multi-messenger era for astronomy. Through an active dissemination programmed, including direct engagement with all relevant stakeholders, and via the development of citizen scientist mass participation experiments, ASTERICS has the ambition to be a flagship for the scientific, industrial and societal impact ESFRI projects can deliver.

VII. EXECUTIVE SUMMARY

This deliverable describes the implementation and realization of a TFT transport service based on White Rabbit over an optical fiber network owned by SURFnet. This type of TFT transport uses a bi-directional connection, where standard fiber networks only use uni-directional connections. Therefore, SURFnet's infrastructure has been changed to accommodate this bi-directional link. The TFT transport service has been implemented on a 169 km optical fiber link including two bi-directional optical amplifiers.

The time and frequency stability of the TFT transport service over a 134 km optical fiber link have been measured and analyzed. Furthermore, all significant delay asymmetries in the optical link have been measured, and agree to within experimental uncertainties with the predicted values. From the results presented, we conclude that the newly provisioned TFT link can support VLBI observations.

1 Table of Contents

2 Abbreviations

ADEV	Allan deviation
BDOA	Bi-Directional Optical Amplifier
C-band	Optical Spectrum between 1525nm and 1565nm
CD	Chromatic Dispersion
CWDM	Course Wavelength Division Multiplexing
DCN	Data Communication Network
DWDM	Dense Wavelength Division Multiplexing
EDFA	Erbium Doped Fiber Amplifier
ENBW	Enabled bandwidth
FOADM	Fixed Optical Add and Drop Multiplexer
LOFAR	Low Frequency Array
MDEV	Modified Allan deviation
MGMT	Management
NOC	Network Operation Center
OMX	Optical Multiplexer
OSC	Optical Supervisory Channel
OTDR	Optical Time Domain Reflectometer
PLO	Phase-Locked Oscillator
PPS	Pulse Per Second
RTT	Round-Trip Time delay
SFP	Small Form-factor Pluggable
SRS	Stanford Research Systems
TFT	Time and Frequency Transfer
TIC	Time Interval Counter
TRX	Transceiver
VLBI	Very-Long-Baseline Interferometry
WR	White Rabbit
WSRT	Westerbork Synthesis Radio Telescope
WSS	Wavelength Selective Switch

3 Introduction

3.1 Motivation and Scope

This deliverable is part of the Cleopatra work package of the ASTERICS project which covers the distribution of time and frequency through public optical fiber for multi-messenger astrophysics, such as very-long-baseline interferometry (VLBI). One of the main aims of this deliverable is to distribute the time and frequency signals of the hydrogen maser located at the Westerbork Synthesis Radio Telescope (WSRT) facility in Zwiggelte to the CAMRAS telescope in Dwingeloo. This will then enable performing VLBI measurements between these two locations, demonstrating the ability to do VLBI using a maser signal distributed over a shared optical network.

3.2 Objective

The objective of this deliverable is to distribute the time and frequency transfer (TFT) of the hydrogen maser at WSRT through a public SURFnet optical fiber network to the CAMRAS telescope. The link length of the fiber link between the CAMRAS telescope and the WSRT facility is extended from a length of 35 km to a length of 169 km by making a 2×67 km loop-back through Groningen. One of the reasons to extend the link is to demonstrate the time and frequency distribution through long-haul optical fiber links. Another reason is to have the possibility to connect the LOFAR network (situated in Groningen) to the TFT distribution. The connection to LOFAR will be part of the future work in this project.

This deliverable describes two main important aspects of the TFT. The first aspect is the realization of the TFT in the public SURFnet optical fiber network. The second aspect is the performance of the TFT in terms of time and frequency stability, and time accuracy.

3.3 Structure

Chapter 4 describes how the TFT between Zwiggelte and Dwingeloo is incorporated in the SURFnet network. Since the start of the project SURFnet, European procurement ruling has forced SURFnet to renew its fiber contracts and introduce a new photonic light system, transponder layer and service layer in its network.

Chapter 5 describes the performance assessment of the 2×67 km TFT optical fiber link between Zwiggelte and Groningen. This assessment includes a discussion of the required and achieved time and frequency stability, and the time accuracy.

Chapter 6 summarizes the work presented in the previous chapters and describes the next steps that need to be taken in this project.

4 Realization of the Fiber and Time and Frequency Transport Infrastructure

This chapter touches on the different aspects that were encountered during the setup of the transport service for the TFT service.

4.1 A New Fiber Plant

Dark-fiber lease contracts are long-term contracts of about 15 years. Shortly after the kick-off of ASTERICS SURFnet was forced to renew these contracts. In most cases contract renewal resulted in continued use of the same dark-fiber service i.e. the same fiber spans remain. In a few cases however, new dark-fibers needed to be procured from a different dark-fiber supplier. This was the case for the Northern branch of the core network.

Figure 4.1 shows the topology of the entire core network. Triangles are in-line amplifiers and squares are add/drop nodes for DWDM waves.

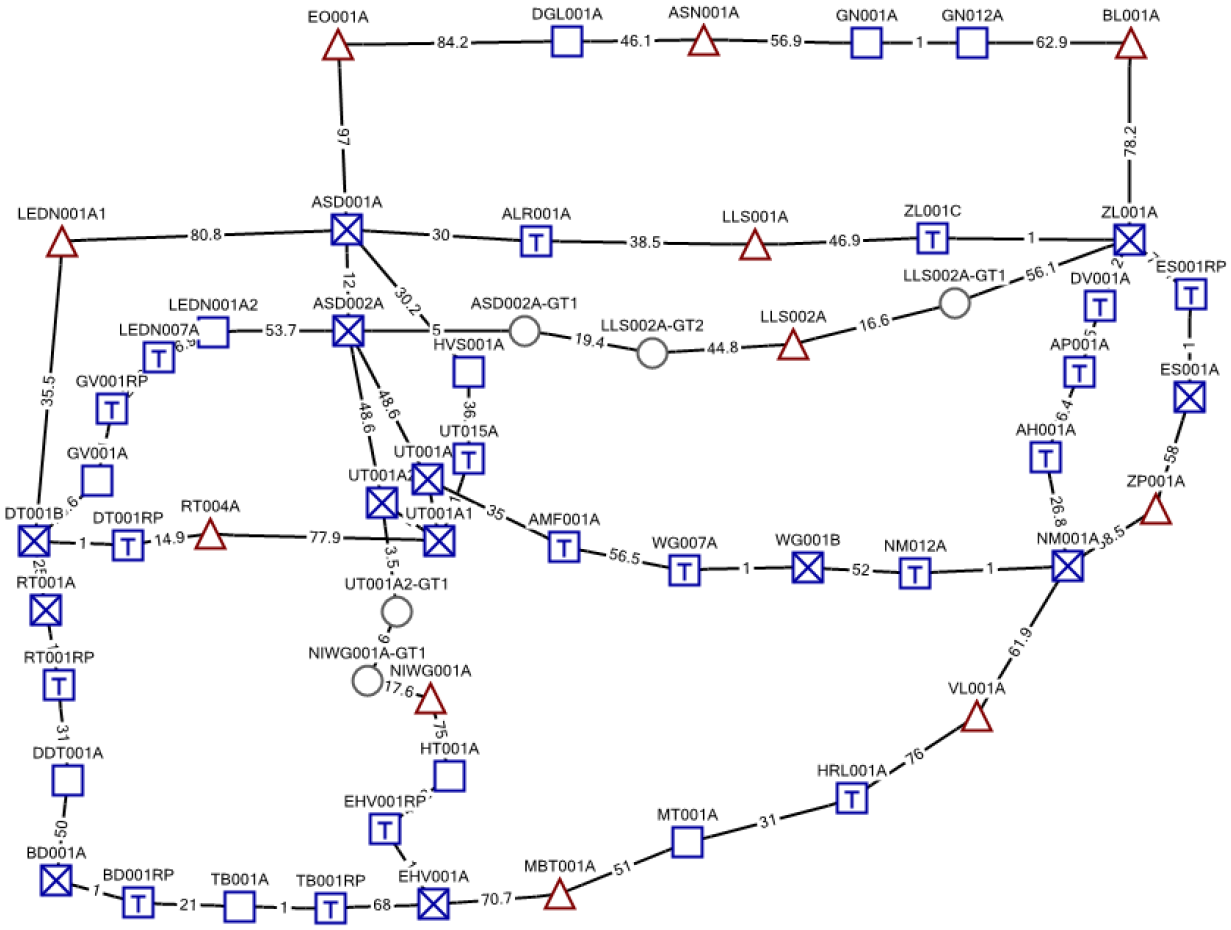

Figure 4.1: Network topology of the core network before fiber renewal

Figure 4.2 shows a close-up of the Northern branch: ASD001A-EO001A-DGL001A-ASN001A-GN001A-GN012A-BL001A-ZL001A. Astron's location in Westerbork (Zwiggelte) was at this point in time not part of SURFnet's network but was connected to the Dwingeloo site via dark fiber put in place when the Dwingeloo site became part of the core network. The LOFAR antenna field in Buinen or Exloo is connected via a dark fiber from LOFAR to SURFnet's GN012A site (University of Groningen). This topology required the following route for the two use cases being the:

1. TFT service between Westerbork and Dwingeloo to go from a master White Rabbit switch in Westerbork to Dwingeloo (where the signal was to be amplified for the first time) and from Dwingeloo to Assen (ASN001A, where a second amplification would take place) and then back to Dwingeloo in order to be terminated on the slave White Rabbit switch.

2. TFT service from Westerbork to Buinen to go from a master White Rabbit switch in Westerbork via Dwingeloo to Assen (ASN001A, where a first-time amplification would take place) and from Assen to GN012A where a second-time amplification would take place before the signal is patched to LOFAR's dark fiber to Buinen/Exloo

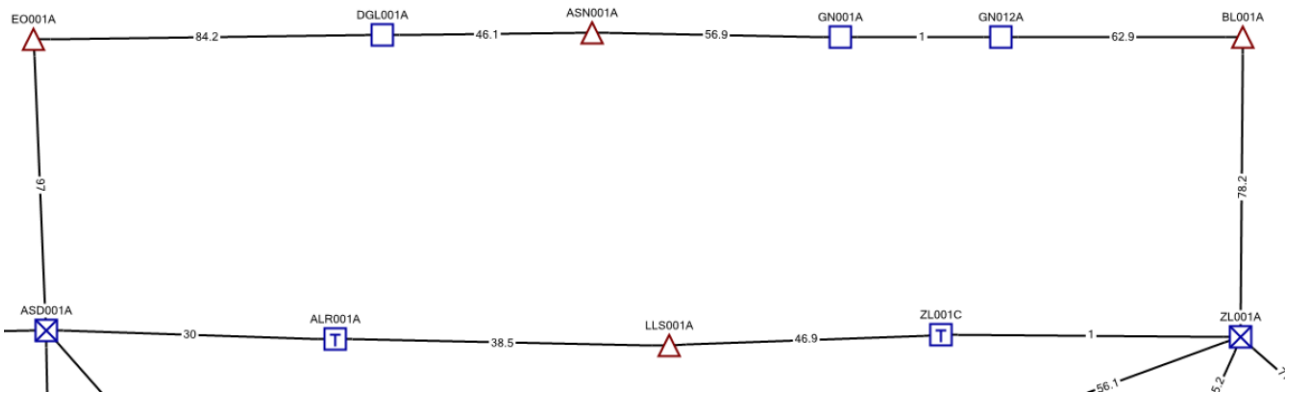

Figure 4.2: Topology of the northern branch (ASD001A-EO001A-DGL001A-ASN001A-GN001A-GN012A-BL001A-ZL001A) of the core network before fiber renewal

When contracts were renewed and new fibers were procured the entire core network was updated. This resulted in the topology as depicted in Figure 4.3. Though large parts remain the same, new branches have been added and in the Northern branch part of a metro ring (MDMR001A-LW001B-GN001A) was absorbed in order to find a solution to connect Dwingeloo as redundant as possible. The new topology of the Northern ring is depicted in Figure 4.4: ASD001A-HN001A-MDMR001A-LW001B-GN001A-GN012A-ZWT001A-DGL001A-MP001A-ZL001A. This new topology results in a different implementation for the two use cases being the:

1. TFT service between Westerbork and Dwingeloo to go from a master White Rabbit switch in Westerbork to Groningen (GN012A, where the signal is to be amplified for

the first time), then back to Westerbork (ZWT001A, where a second amplification takes place) and then to Dwingeloo in order to be terminated on the slave White Rabbit switch.

2. TFT service from Westerbork to Buinen to go from a master White Rabbit switch in Westerbork directly to Groningen (this is now possible) (where amplification takes place) and where the amplified signal is patched to LOFAR's dark fiber to Buinen/Exloo.

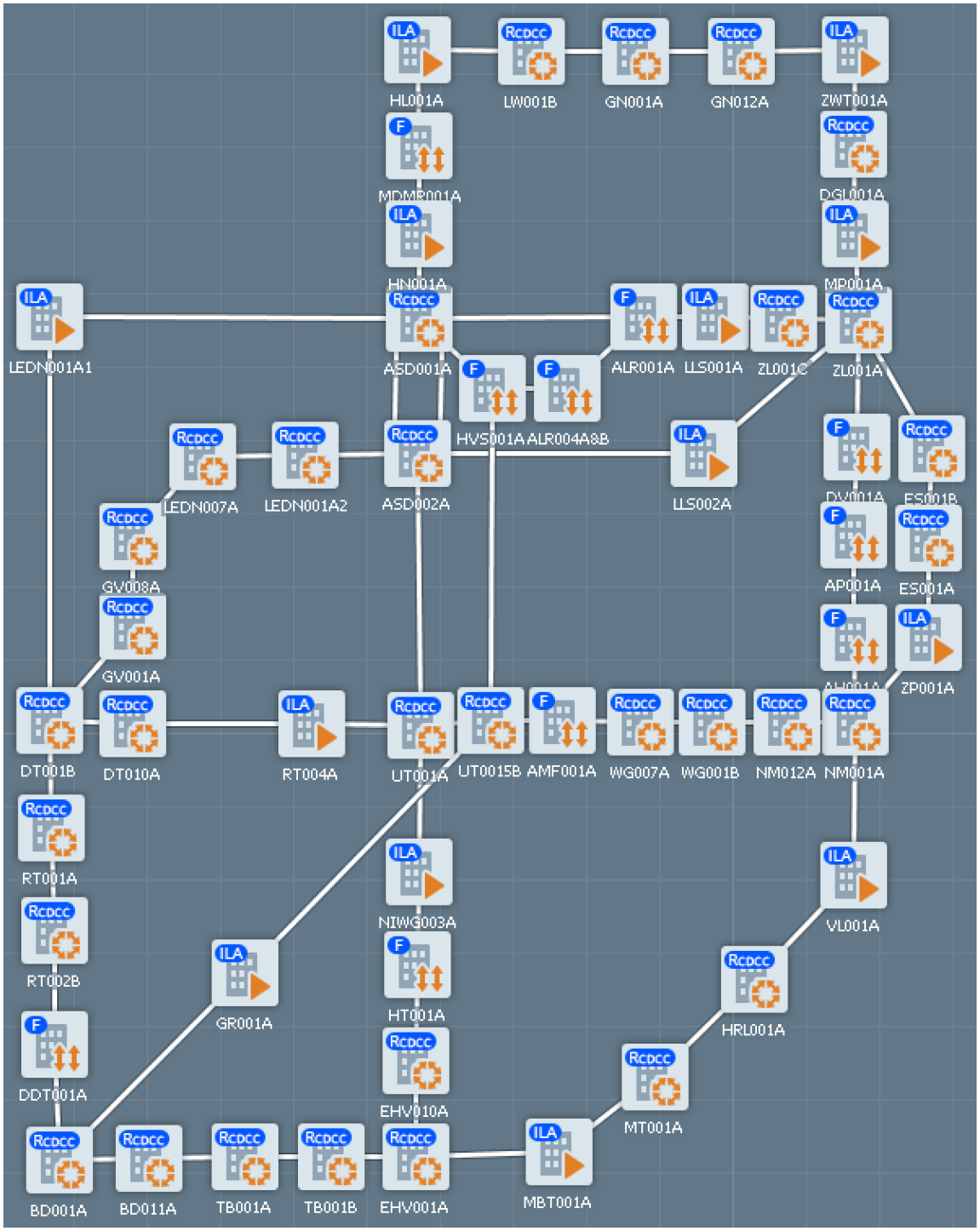

Figure 4.3: Network topology of the core network after fiber renewal

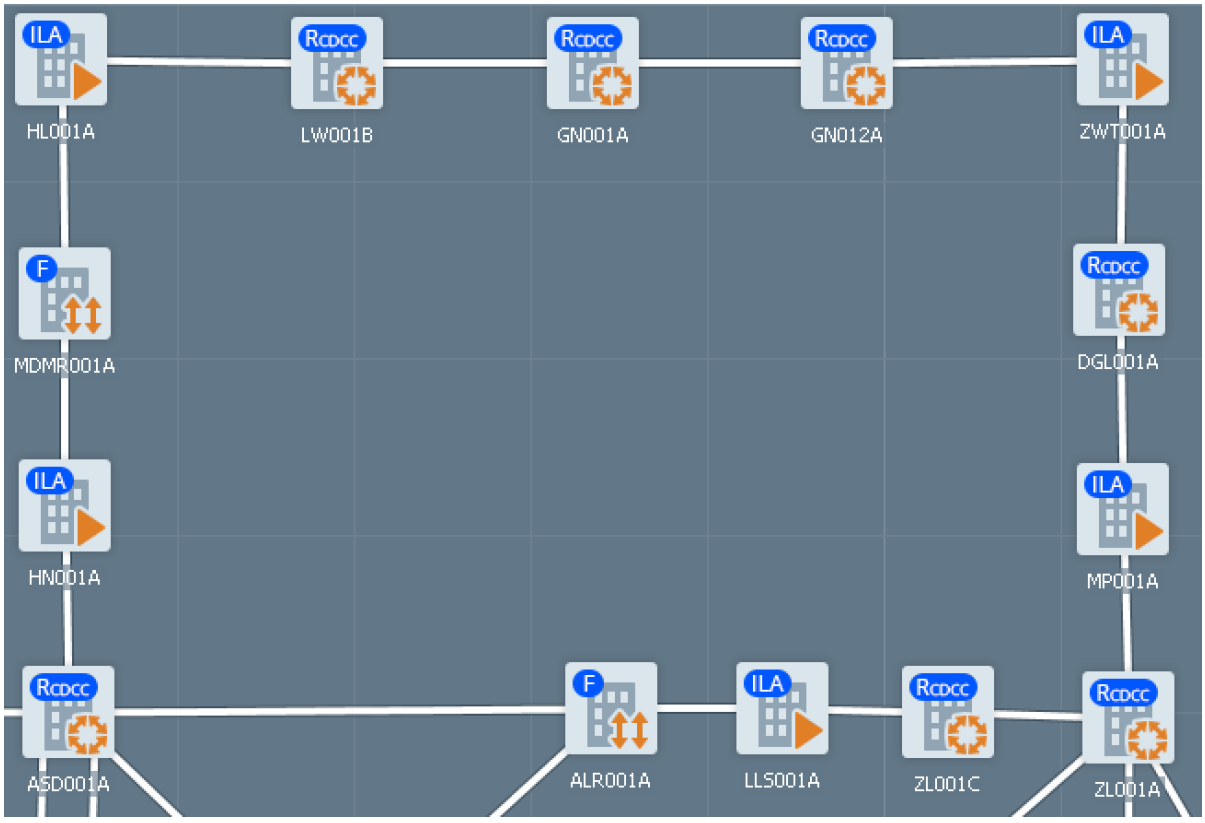

Figure 4.4: Topology of the northern branch (ASD001A-HN001A-MDMR001A-HL001A-LW001B-GN001A-GN012A-ZWT001A-DGL001A-MP001A-ZL001A) of the core network after introduction of new fiber spans

4.2 A New Light System

The fiber renewal in the Northern branch of the network coincided with the renewal of the Photonic Light System. In 2016 a public procurement was issued and in this public procurement SURFnet requested a solution that would allow, in addition to regular transport services in the C-band, other photonic services to coexist with the transport system. As an example, SURFnet used the TFT service and asked integrators for a solution in an awarding requirement. This section outlines how (in terms of components) the awarded solution has been adopted to combine a production grade carrier service with other services.

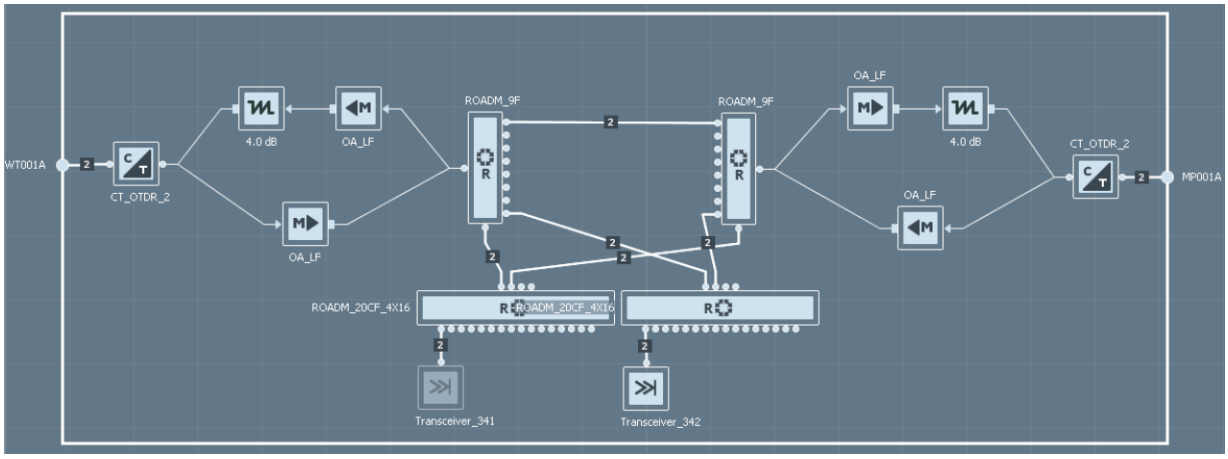

Figure 4.5: Design of the photonic node (Colorless-Directionless-Contentionless Reconfigurable Optical Add and Drop Multiplexer) at Astron (DGL001A) between the sites ZWT001A and MP001A. The design of the node at GN012A is identical to this node.

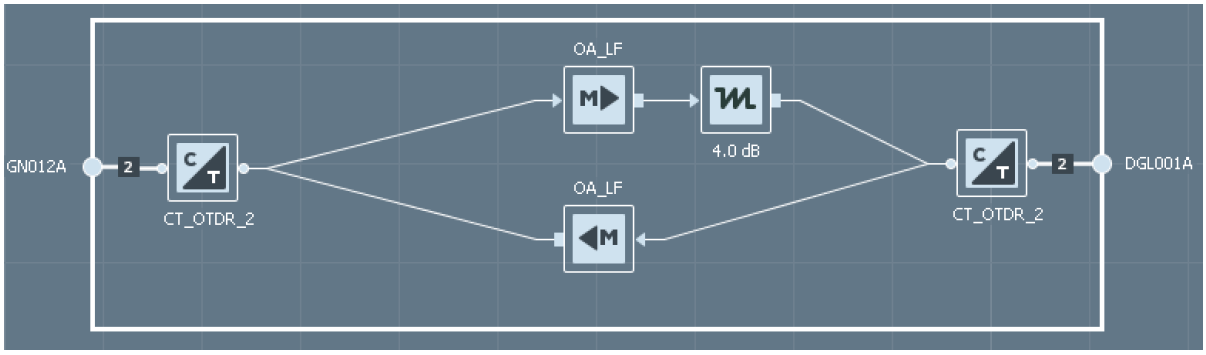

Figure 4.6: Design of the photonic node (In-Line Amplifier) at the Westerbork site (Zwiggelte, ZWT001A) between GN012A and DGL001A

Figure 4.5 and Figure 4.6 show the interior of the nodes GN001A, DGL001A, and ZWT001A schematically. For every outgoing line fiber a filter has been implemented, which combines DWDM waves in the C-band with the 1610nm CWDM band and other waves presented on the "OSC-1510 WIDE" port. This filter is present on all core nodes in the network and allows in addition to C-band transport service other photonic services to be injected on the 1610nm port or on the "OSC-1510 WIDE" port. Figure 4.7 shows a picture of a filter module containing two of these CT_OTDR filters.

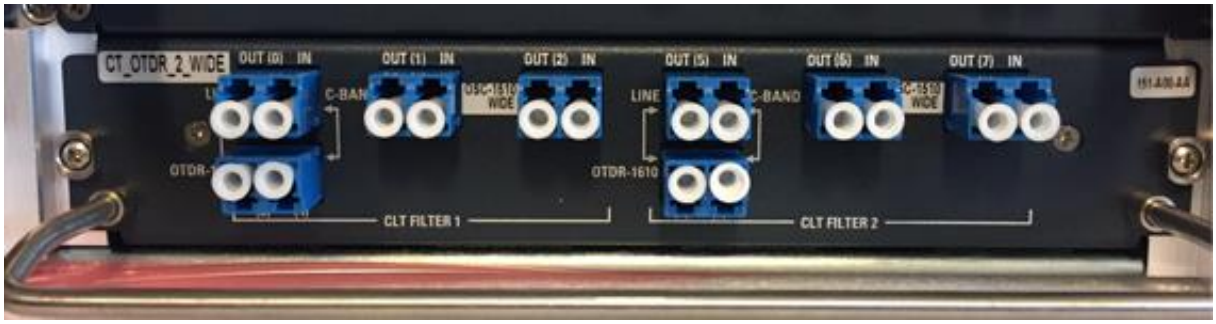

Figure 4.7: Filter for multiplexing different type of photonic services onto a line fiber. Two of these filters are combined in one swappable module. For each filter: the top-left port is where the line fibers connect, the middle top port is for the C-band waves, the top right port is for the OSC 1510nm and other photonic services, and finally the bottom left port is for the 1610nm band often used for OTDR measurements.

4.3 Architectural Impact for the TFT Service

With new fibers and a new-generation light system, the TFT service can now be implemented significantly easier than was the case in the old infrastructure, which was presented in ASTERICS Deliverable D5.1. Figure 4.8 shows the architecture of how the TFT service can be added to a DWDM environment. Even in the case of the wavelength of the TFT signals are placed inside the C-band, the line filter can be customized in support of such a scenario.

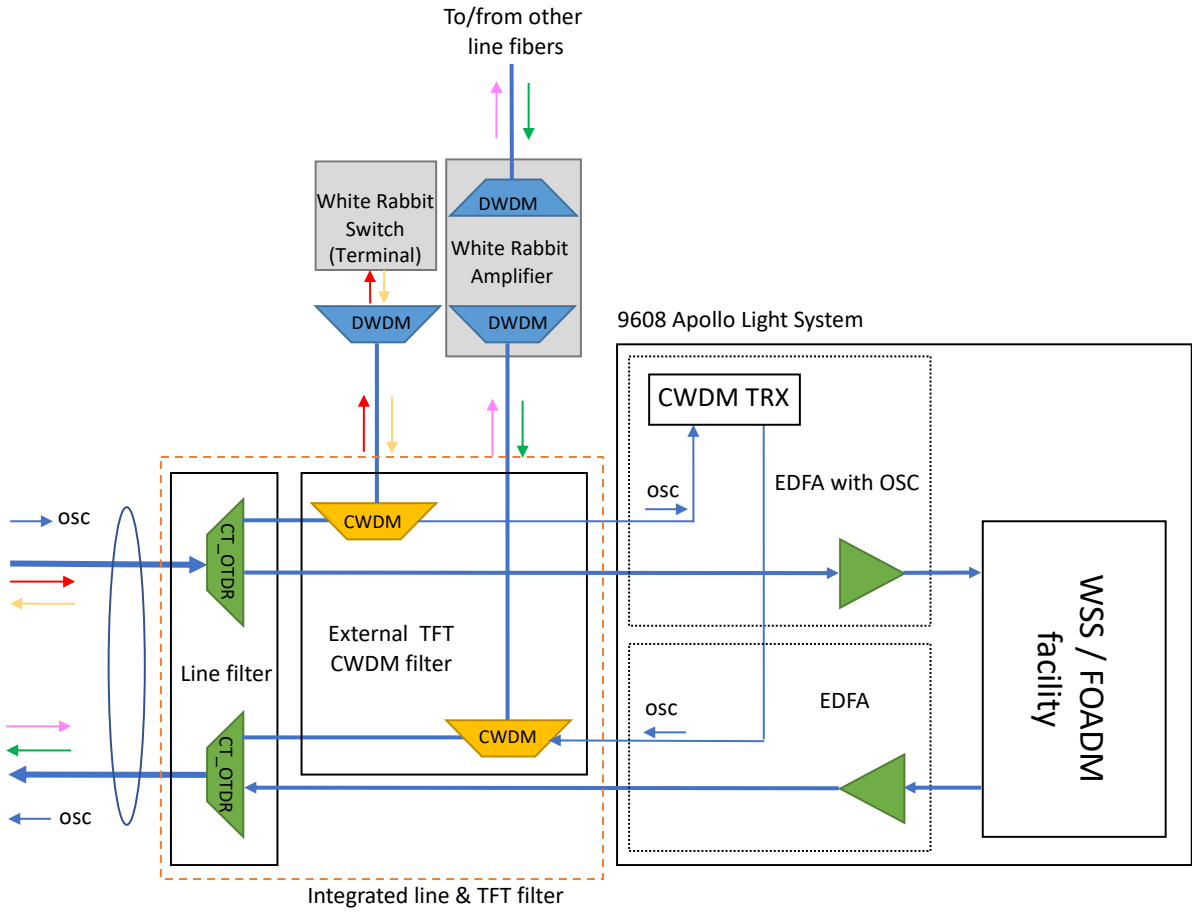

Figure 4.8: The newly purchased light system allows for a custom designed line filter. TFT services can be added using an external TFT CWDM filter or in case of large-scale roll-out existing filters can be retrofitted with filters, which are required for the service.

4.4 Staging at SURFnet HQ

Before the TFT equipment is installed in the field, the equipment was staged at SURFnet headquarters. Figure 4.9 and Figure 4.10 show the installation of a master and slave switch and two optical amplifiers. The attenuation of the transmission fiber was emulated using attenuators (pads). The design of the staging matched the design of the link as it was installed and lined-up (Section 4.5)

The objective of the staging process was to be able to configure the equipment and to adjust padding in such a way that power levels at the input and output of the amplifiers and switches are within acceptable range. It also provided means to understand and learn the command line interface.

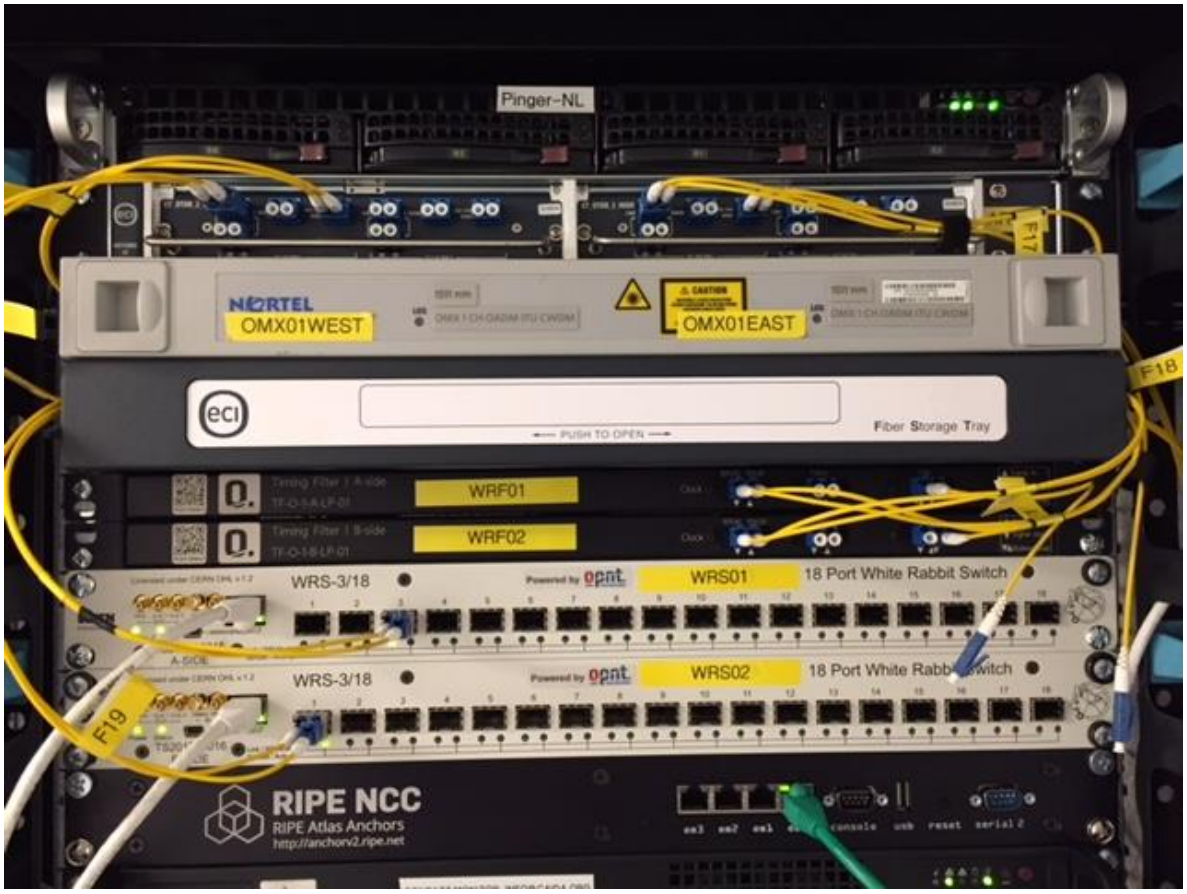

Figure 4.9: Staged White Rabbit nodes in the main equipment room at SURFnet headquarters in Utrecht. Both Master (WRS01) and Slave (WRS02) and associated multiplexers (WRF01 and WRF02), two 1510nm CWDM filters (OMX01WEST and OMX01EAST) and the CT_OTDR filters have been placed together for convenience.

During staging the impact of the polarization sensitivity of the amplifiers was also verified and found that this would not impact the field deployment as gain saturation would dampen polarization-sensitivity induced power fluctuation.

4.5 Installation and Line-Up

On four different sites and in three different domains installations need to take place. Figure 4.11 shows the schematic installation in Westerbork (Zwiggelte, ZWT001A) in both SURFnet's domain and the customer's domain (dotted red box). Figure 4.13 shows the implementation in Groningen (GN012A), this is entirely SURFnet's domain. A patch has been implemented to allow the TFT service to be terminated in Dwingeloo or on a dark fiber terminating on a White Rabbit switch in the LOFAR antenna field in Buinen/Exloo. Figure 4.14 displays the installed configuration in Dwingeloo (DGL001A). Also, here the amplifier is placed in SURFnet's domain, while the White Rabbit slave switch is placed in the domain of the customer. Figure 4.15 shows

the installation that must take place at ASTRON's location in Buinen/Exloo where time can be delivered to the receiving antenna signal processing electronics.

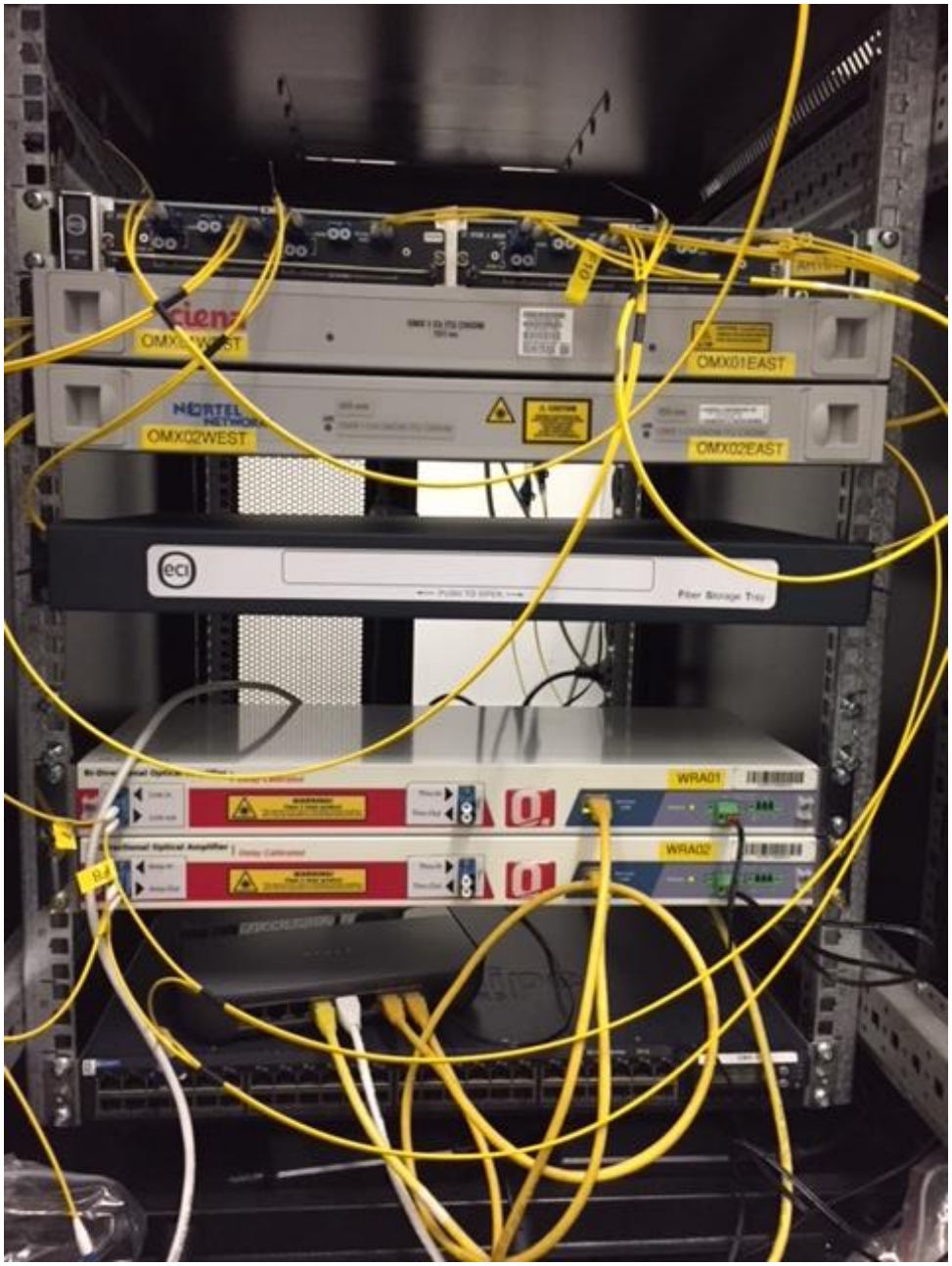

Figure 4.10: In SURFnet's demo room two bi-directional amplifiers were placed, also with all required filters.

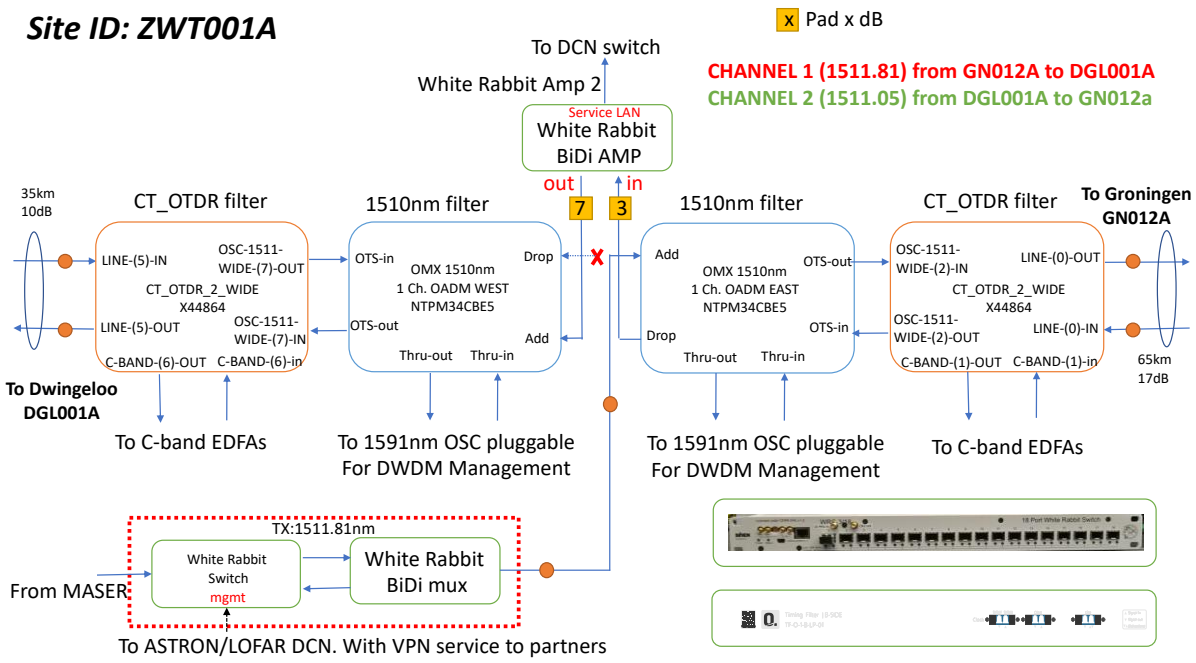

Figure 4.11: Implementation of the White Rabbit based TFT link at Zwiggelte (ZWT001A)

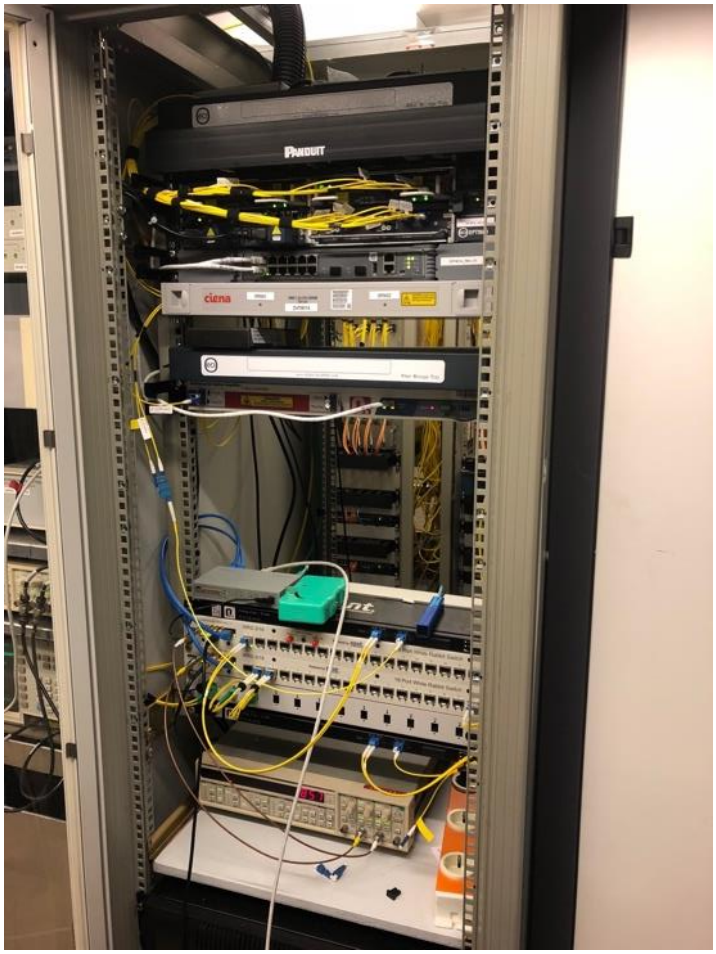

Figure 4.12: Zwiggelte Installation and line-up in progress. From top to bottom: Fiber management tray, Panduit fiber guide, Repeater for C-band transport services and CT_OTDR filter (See Figure 4.6), DCN switch, OMX filter for adding and dropping the TFT signals, Empty slot, Fiber management tray, Bi-Directional Optical Amplifier for TFT service, Bi-directional multi-demultiplexer for TFT service (black box), 2x White Rabbit switch, 2x bi-directional multi-demultiplexer (beige and black box). On the plateau a timer is placed and connected to the White Rabbit switches for path delay measurements.

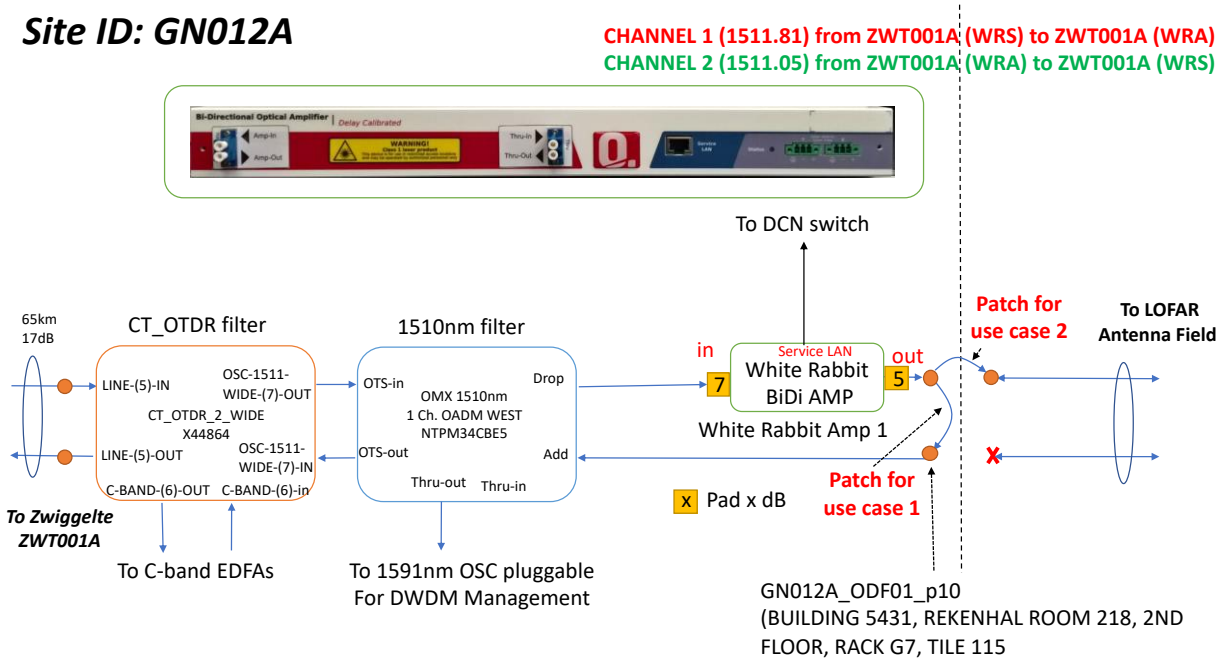

Figure 4.13: Implementation of the White Rabbit based TFT link at Groningen (GN012A). Depending on the patch cable the service is delivered at the LOFAR antenna field in Buinen/Exloo or delivered at Dwingeloo (DGL001A)

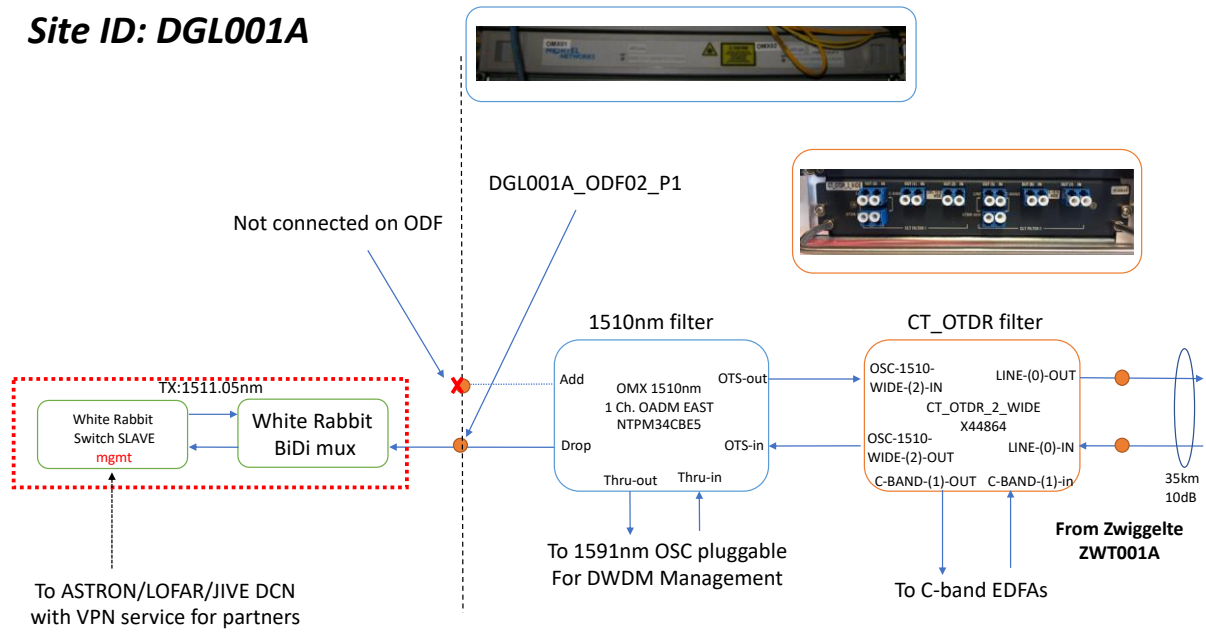

Figure 4.14: Implementation of the White Rabbit based TFT link at Dwingeloo (DGL001A)

LOFAR Site at Buinen/Exloo

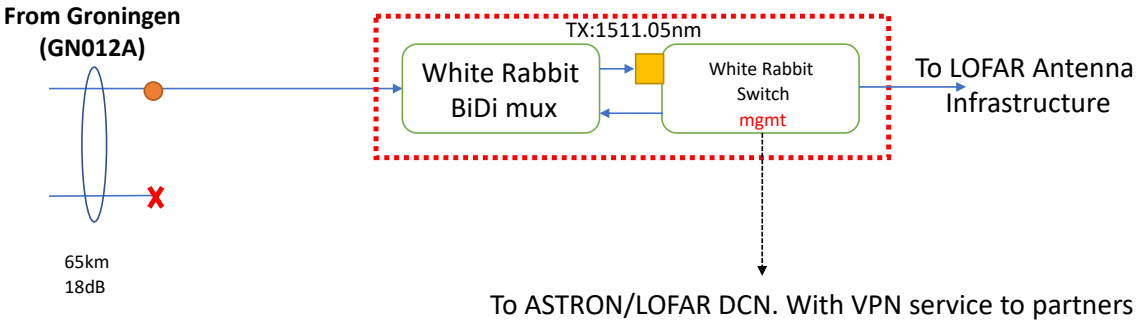

Figure 4.15: Implementation of the White Rabbit based TFT link termination at the LOFAR Antenna Site at Buinen/Exloo.

4.6 Lessons Learnt and Best Practices for Future Roll-Outs

The following lessons have been learnt:

- New generation photonic light systems are much more open in supporting (niche) photonic services.
- Attenuation at the amplifier ports is most convenient when one assumes equal span attenuations.
- In the case more than two amplifiers are daisy chained, amplifiers must not be operated in a constant gain mode anymore. For these deployments power control per channel is required.
- Field engineering did not have any issues installing the equipment and connecting it correctly to the existing infrastructure (DWDM equipment and 1510nm OMX CWDM filters)

During the staging, installation and commissioning, the following best practices have been identified:

- Because light travels bi-directionally in a single fiber for this service and passes through ports that assume uni-directional light, it is important to establish a convention. Following the direction of time transfer, the wave from master to slave enters all devices with uni-directional port naming in the normal fashion (wave enters a device on the “add”, “in”, “RX”, “thru-in” port and leaves a device on the “drop”, “out”, “TX”, “thru-out” port.
- When attenuators are added to a span to meet equal amplifier gain per span, it is preferred to place half of the attenuation on each end of the span. This lowers power everywhere on the fiber and reduces non-linear noise as well as in-elastic scattering.

- In this case the TFT service has been implemented as a bi-directional alien wave service over the operator's network. This works best if the White Rabbit switches are under the control of the customer and the amplifiers under the control of the operator. The latter is important as the operator can verify the amount of power launched in the fiber. This mode of operation can only be supported for friendly and knowledgeable customers and end-users. In all other cases the TFT service will be made available electrically (10MHZ and 1PPS signals) and the operator also manages the White Rabbit master and slave switches.

5 Performance Assessment of 2x67 km Multiplexed WR Link

To build a TFT link between the WSRT telescopes and the CAMRAS telescope in Dwingeloo, the existing direct optical fiber link with a length of 35 km would cover the distance between the two sites. However, for demonstration purposes the optical fiber link is extended with a loop-back from Zwiggelte to Groningen back to Zwiggelte, before the TFT signal is sent to Dwingeloo (see Figure 5.1). This extra 2x67 km of optical fiber makes the total distance of the optical fiber link 169 km. By using this extended optical fiber link, the aim is to demonstrate that the distribution of time and frequency through public optical fiber networks for VLBI is feasible, even for distances up to 169 km.

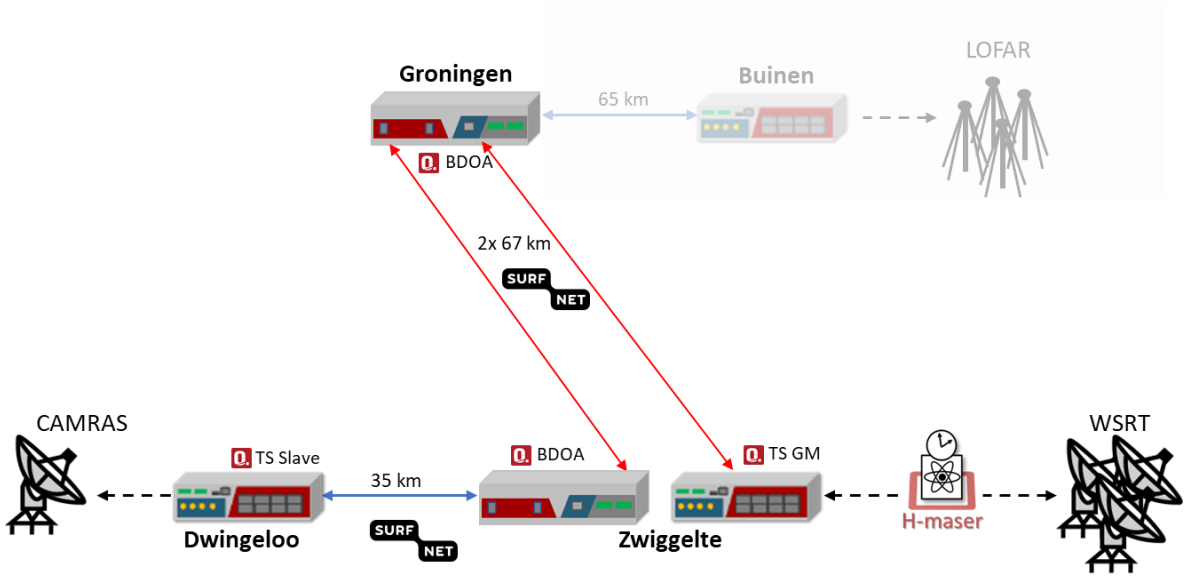

Figure 5.1: Overview of the locations that are used in the TFT link between Zwiggelte and Dwingeloo through Groningen. The time and frequency signals of the hydrogen (H-) maser located at the WSRT telescopes will be distributed to the CAMRAS telescope to synchronize the CAMRAS telescopes with the WSRT telescopes. In a later stage of the project LOFAR will also be included in the TFT distribution.

OPNT Timing Switches are used to transfer the time and frequency signals through the optical link, making use of the White Rabbit (WR) protocol [1]. These are White Rabbit switches compliant with v3.4 release on the OHWR repository, with added low-jitter daughter boards. The slave switch furthermore has been fitted with a clean-up oscillator with a very low phase noise [2]. The grand master Timing Switch (TS GM) is directly synchronized to the hydrogen maser at WSRT, while the slave Timing Switch (TS Slave) at Dwingeloo is synchronized to the TS GM using the WR protocol through the public SURFnet optical fiber network. The TFT signals are optically amplified in Groningen and Zwiggelte using dedicated OPNT Bi-Directional Optical Amplifiers (BDOAs).

To directly measure the time and frequency stability of the TFT link, it is required to have the TS GM and TS Slave at the same location. Therefore, during the performance measurements we temporarily move the TS Slave from Dwingeloo to Zwiggelte and remove the BDOA in Zwiggelte. This means that the TFT link under test covers a total optical fiber length of 134 km (indicated by the red lines in Figure 5.1), leaving out the optical fiber link to Dwingeloo. The details of the measurement setup and the time and frequency stability measurement results can be found in Section 5.1 and Section 0, respectively.

The absolute phase difference between the TS GM and TS Slave is determined by all temporal delay asymmetries between the upstream signal (TS GM → TS Slave), and the reverse downstream signal. This phase difference partly originates from path delay asymmetries, *i.e.* caused by different fiber lengths in the optical filters and BDOAs, and internal electrical path delay asymmetries in the Timing Switches. Another contribution to the phase difference is related to the chromatic dispersion (CD) of the long-haul fiber links, which will cause a differential link delay asymmetry since WR makes use of different upstream and downstream wavelengths. Section 0 describes all measured and estimated delay asymmetries in the test setup.

5.1 Requirements for VLBI Time and Frequency Transfer

For most of the past half century of VLBI, the Hydrogen maser has been the only reference source with sufficient stability to support VLBI at microwave frequencies. We perform a simple analysis of the required coherence to show the required stability for VLBI, based on recent design work carried out for the SKA [3].

VLBI requires a sufficiently stable reference frequency such that during an integration (on the order of a second to a minute), the coherence between the recorded signals from the participating observatories is not significantly reduced. Somewhat arbitrarily, we put those limits at 2%, as used in the SKA case. For a clock with a white phase noise spectrum (which has a slope of -1 in the ADEV), this corresponds to 0.2 radians RMS phase noise. The coherence loss can be expressed as

$$L = 1 - \sqrt{e^{-\frac{4\pi^2}{3}\sigma_y^2 \tau^2 v_0^2}}$$

with σ_y^2 the Allan variation (at $\tau = 1$ s), τ the observation time (in s) for this value of the AVAR (hence 1 s), and v_0 the observing frequency (in Hz). Note that in the case of white phase noise, the correlation loss does not depend on the integration time.

The Dwingeloo telescope is currently equipped to observe around 430 MHz and 1400 Mhz. The mesh of the main reflector is capable of supporting observations up to about 6 GHz, at shorter wavelengths the mesh becomes transparent to the radio signal. After rewriting the

formula and substituting 2% coherence loss and a highest observing frequency of 6GHz, we find a required ADEV of 9×10^{-12} at $\tau = 1$ s. For observing at 1400MHz, the required ADEV would be 4×10^{-11} at $\tau = 1$ s.

Phase referencing (switching between observing the source and a nearby phase calibrator to reduce the effects of the changing ionosphere) requires that there should be no phase ambiguity when connecting the phase signals over the switching interval, which is on the order of 5 minutes. At 6 GHz, a single phase corresponds to 166 ps. To prevent ambiguities, the timing changes on the timescale of 5 minutes should therefore be less than 84 ps, so the phases from reference scans can be connected together.

Most VLBI networks will observe a compact, bright object at the start of an observation to establish the clock differences between all participating stations. It is convenient for the offset to be less than approximately 15 µs (512 lags in a 16 MHz sub-band) so that the fringe is immediately apparent during this clock searching operation.

5.2 Measurement Setup

Figure 5.2 shows a schematic of the setup that is used to test the accuracy and stability performance of the TFT signals. For simplicity, the SURFnet optical network is represented by the "OSC + C-band" block without explicitly showing all optical components. The extended lay-out of the optical fiber network can be found in Chapter 4. A picture of the setup in Zwiggelte and a picture of the hydrogen maser can be found in the Appendix, Figure 0.1 and Figure 0.2.

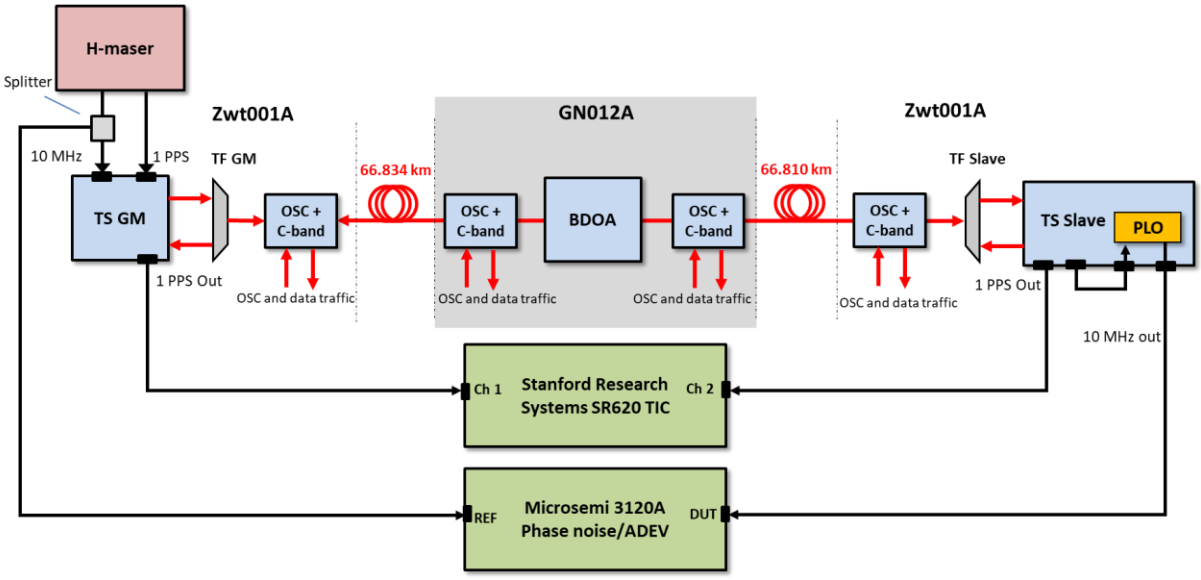

Figure 5.2: Simplified schematic of the TFT from Zwiggelte (Zwt001A) to Groningen (GN012A) back to Zwiggelte, including two OPNT Timing Switches (TS GM and TS Slave) and one OPNT BDOA. A Microsemi 3120A and an SRS SR620 are used to measure the performance of the TFT link in terms of timing accuracy and time and frequency stability.

The TS GM is directly referenced to the hydrogen maser using a 1 PPS and 10 MHz signal. The TS Slave is synchronized to the TS GM through the optical fiber network using the WR protocol. To obtain the best TFT performance, a bi-directional link is used where the optical signals from the TS GM and TS Slave are transmitted into the same optical fiber in opposite directions. The optical signals are multiplexed and de-multiplexed at the beginning and end of the link using OPNT Timing Filters (TF GM and TF Slave). Furthermore, the bi-directional TFT signals are amplified in Groningen using an OPNT Bi-Directional Optical Amplifier (BDOA).

Both timing switches contain a low-jitter daughterboard to reduce the phase noise jitter [2, 4]. In addition, the TS Slave includes a phase-locked oscillator (PLO) with a 1 Hz PLL bandwidth to further clean-up the low-frequency phase noise of the 10 MHz output of the switch [2]. The 10 MHz output from the hydrogen maser and the 10 MHz output from the TS Slave are directly compared using a Microsemi 3120A phase noise test probe. The 1 PPS signals from the two timing switches are compared using a Stanford Research Systems (SRS) SR620 time interval counter (TIC). A list of all equipment is presented in the Appendix, Table 0.1Table 0.1.

A small form-factor pluggable transceiver (SFP) is used in each Timing Switch to transmit and receive the TFT signals. The SFPs are compliant with a 100 GHz DWDM grid. The transmitted wavelength from the TS GM is 1511.81 nm, whereas the transmitted wavelength of the TS Slave is 1511.05 nm.

5.3 Time and Frequency Transfer Stability Results

A five-day measurement is performed where the phase differences between the 10 MHz signals and the 1 PPS signals are logged using the setup as depicted in Figure 5.2. The results are shown in Figure 5.3 in which the red lines represent the raw data and the blue lines represent the data averaged over 100 samples. The 1 PPS phase difference measurement is limited by the 20 ps jitter of the SR620 TIC. Averaging the data reveals the long-term variation of the phase difference between the two 1 PPS signals, which is in accordance with the long-term phase difference variation measured with the 10 MHz signals.

Figure 5.4 shows the Allan deviation (ADEV) and modified Allan deviation (MDEV) of the TFT link. The ADEV that is obtained with the 1 PPS phase difference measurements (green curve) is dominated by the phase jitter of the SR620 counter. The $\tau^{-3/2}$ slope of the accompanying MDEV reveals that the SR620 counter produces white phase modulated noise. The MDEV also shows that the frequency stability for averaging times > 300 s overlaps with the frequency stability of the 10 MHz phase difference (blue curve), averaging down to 1.5×10^{-16} at 10^5s.

The long-term variation in the phase difference that is observed in the temporal phase difference data (Figure 5.3) can also be seen in the ADEV/MDEV at 5000 s where the frequency stability curve levels off. These phase variations may be explained by wavelength drifts of the optical transmitters that are used [2, 5]. A temporal variation in the transmitted wavelength

results in a variation of the link asymmetry caused by CD, leading to a varying phase difference between the TS GM and TS Slave. For example, a variation of 0.02 nm between the two optical transmitters over the 134 km link with a realistic CD of 12.5 ps/(nm km) (see Table 5.3), would already lead to a phase difference of ~30 ps. This would cause a frequency error in the order of 10^{-15} at 5000 s. To test whether this effect is really the cause of the variations as observed in Figure 5.3, the wavelength of the transmitters should be measured versus the temperature of the transmitter and the phase difference between the Timing Switches.

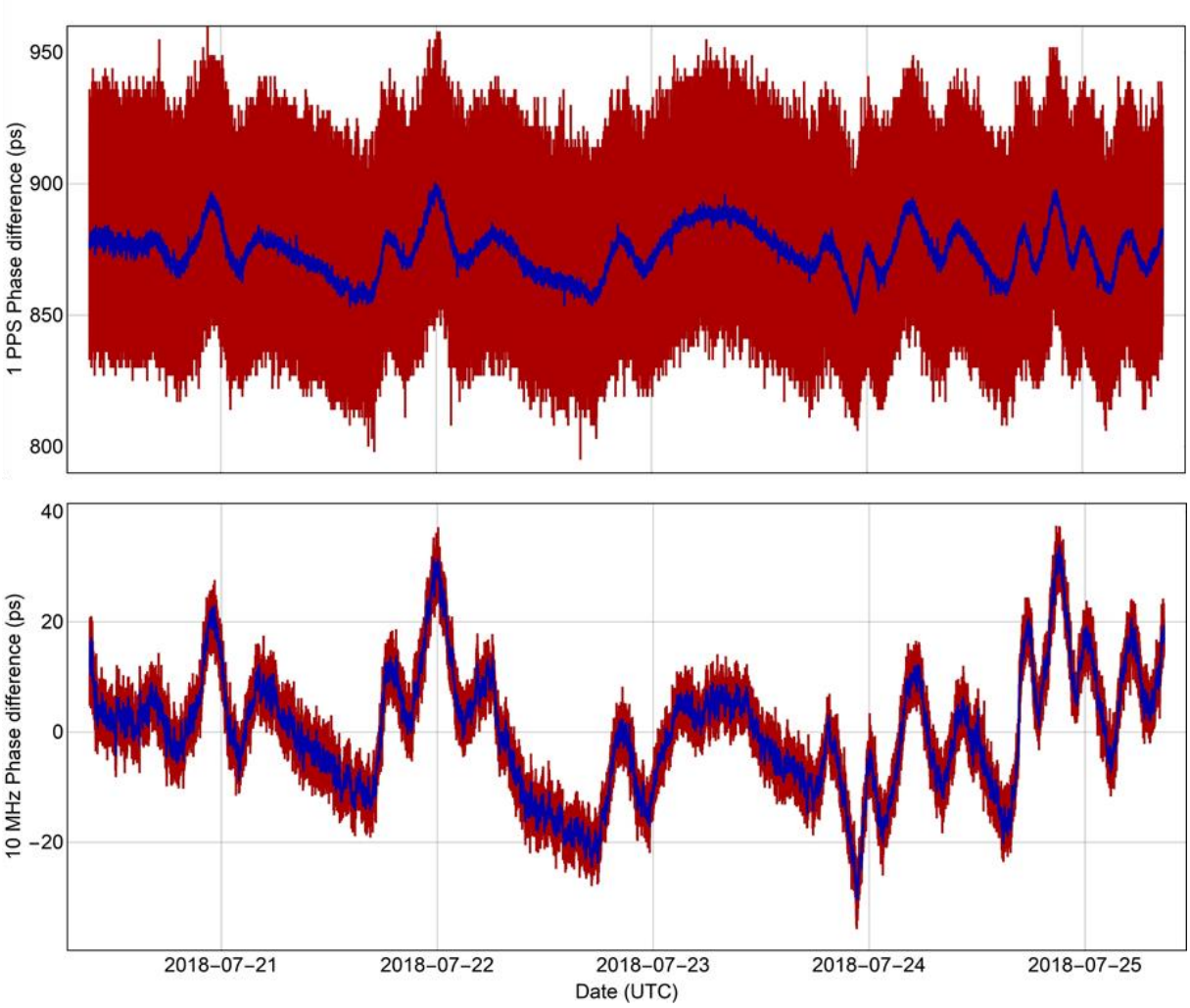

Figure 5.3: Five-day time (top) and frequency (bottom) comparison between the TS GM and the TS Slave, covering an optical fiber length of 134 km, several optical filters, and one BDOA. The frequency data is obtained with an enabled bandwidth (ENBW) of 0.5 Hz. The red data shows the raw data obtained by the measurement devices, where the blue data is given by averaging over 100 samples. The averaged data clearly shows that the 1 PPS and the 10 MHz signals encounter the same temporal variations.

To determine whether the TFT link could be used to distribute a frequency signal with sufficient stability to perform VLBI observations, we compare the frequency stability of the

TFT link with the requirements derived in section 5.1. There we assumed white phase noise behavior, and the ADEV plots indeed match well with a slope of -1, and an intercept of about 3×10^{-12} at τ = 1s. This actually overestimates the noise between 1s and 20 s slightly. Given the required ADEV values of 9×10^{-12} (6GHz) and 4×10^{-11} (1.4 GHz) there should be no significant loss of coherence due to the TFF link. Note that the achieved coherence will also be affected by ionospheric and tropospheric variations, as in any VLBI observation. Figure 5.3 shows that the stability requirement of 84 ps in 5 minutes is also met, as even in the full 5 days of measurement, the timing offsets stay within 80 ps.

We also compare our results to the quoted stability of a commercially available active hydrogen maser. The manufacturer's specification of a modern hydrogen maser is used (Microsemi MHM 2010 standard option, see Figure 5.4) to make a fair and realistic comparison. Note, that we can only directly compare the hydrogen maser ADEV data obtained with an enabled bandwidth (ENBW) of 0.5 Hz, with the ADEV data of the TFT link that is also obtained with a 0.5 Hz ENBW. These measurements are represented by the black and red curve in Figure 5.4, respectively. By comparing these two curves, we can conclude that after an averaging of 1000 s, the frequency stability of the TFT link is already within two times the frequency stability of a brand-new hydrogen maser.

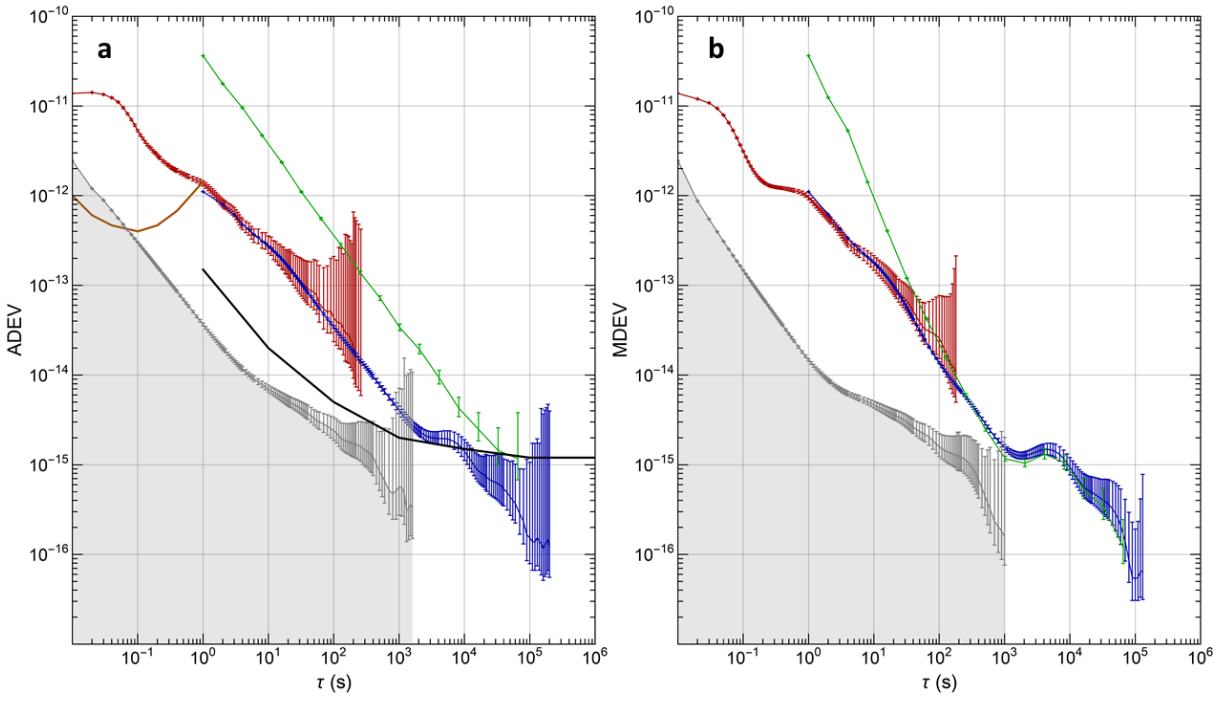

Figure 5.4: Long-term frequency stability of WR over 134 km of optical fiber including optical amplification of one BDOA (see also Figure 5.2). (a) ADEV results and (b) MDEV results: red curve, 10 MHz comparison (50 Hz ENBW, 60 000 samples); blue curve, 10 MHz comparison (0.5 Hz ENBW, 429 860 samples); green curve, 1 PPS comparison (502 000 samples); brown curve, PLO frequency stability according to the datasheet (500 Hz ENBW); black curve, active hydrogen maser (0.5 Hz ENBW); grey curve, Microsemi 3120A noise floor.

The short-term frequency stability (0.01 s – 1 s) of the TFT link is considered to be dominated by the performance of the PLO that is controlled with a 1 Hz PLL bandwidth, with the

assumption that the short-term stability of the hydrogen maser is better than that of the PLO. However, the red curve in Figure 5.4 shows that the measured short-term frequency stability is at least one order of magnitude higher than the expected performance given by the PLO (brown curve in Figure 5.4). Further investigation was needed to reveal which oscillator, the hydrogen maser or the PLO, caused the degraded short-term frequency stability of the TFT link. Hence, we measured the performance of both oscillators against a third oscillator, an SRS Rubidium clock. The ADEV and phase noise power spectral density results are shown in Figure 5.5. By comparing these three measurements it can be concluded that the hydrogen maser adds significantly more short-term frequency phase noise than both the PLO and the Rubidium clock add. These results have been shared with the WSRT facility for further research on the performance of their hydrogen maser.

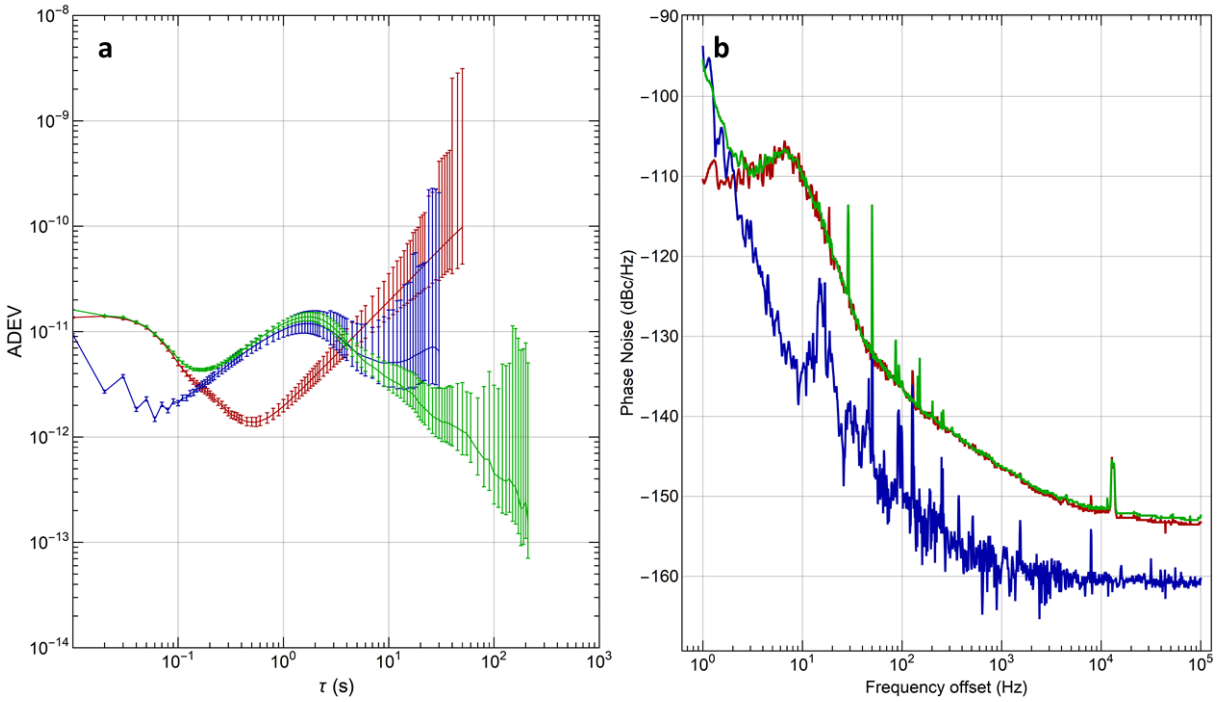

Figure 5.5: (a) ADEV with 50 Hz ENWB and (b) phase noise power spectral density (b) of the comparison between the 10 MHz frequency outputs of two oscillators: blue, Rubidium clock versus PLO; red, hydrogen maser versus PLO; green, hydrogen maser versus Rubidium clock.

5.4 Delay Asymmetry Calibration

This section describes three different delay asymmetries that all add up to the total phase difference between the TS GM and TS Slave. One of the delay asymmetries originates from the optical (de-) multiplexers in the fiber link. The OPNT Timing Filters and OPNT BDOAs contain these (de-)multiplexers that split/combine the upstream and downstream WR signals. Due to an optical path length differences between the fibers that are used for the upstream and downstream signals, these devices cause a link delay asymmetry which result in a phase

difference between the TS GM and TS Slave. The delay asymmetries of these filters and optical amplifiers where measured before installing the devices in the optical network. Here, the asymmetry is defined as

$$\Delta = \frac{\delta_{\text{upstream}} - \delta_{\text{downstream}}}{2}, \qquad [1]$$

where δ_{upstream} is the absolute time delay of the upstream signal through the device and similarly $\delta_{\text{downstream}}$ is the absolute time delay of the downstream signal. The uncertainty[1] in the asymmetry values is given by the standard deviation, rather than the standard error. To properly estimate the uncertainty, all systematic and random uncertainties of the calibration setup would have to be estimated. One of these uncertainties that is not fully estimated derives from the OPNT Timing Switches that are used to measure the time delays, δ. Therefore, to not underestimate the uncertainty, we choose to report the standard deviation instead of the standard error. Table 5.1 lists the measured asymmetries of all the equipment in the measurement setup (Figure 5.2).

Table 5.1: Asymmetries of the Timing Filters and BDOA in the measurement setup.

Device	Δ (ps)	Uncertainty (ps)
TF GM	-38	12
TF Slave	-53	11
BDOA	791	20[2]

Second, the internal delay differences in the TS GM and TS Slave also contribute to the phase difference between the two Timing Switches. Figure 5.6 (a) shows the experimental setup that is used to measure the asymmetry caused by these internal delays. The SR620 TIC measures the phase difference between the TS GM and TS Slave while the two Timing Switches are connected with a short duplex fiber patch cord and suitable attenuators to prevent damage to the SFPs. The delay asymmetry of the patch cord can be neglected. The asymmetry caused by the Timing Switches, Δ_{TS}, is found to be (-356 $\pm$ 20) ps[3]. The uncertainty in this measurement is dominated by the jitter of the SR620 counter.

The third contribution to the phase difference between the Timing Switches is caused by the CD of the long-haul optical fiber link. Figure 5.6 (b) shows the experimental setup that is used to determine this third contribution. The phase difference that is measured by using this setup is given by the sum of all asymmetries in the link:

$$\Delta = \Delta_{\text{TF GM}} + \Delta_{\text{TF Slave}} + \Delta_{\text{BDOA}} + \Delta_{\text{TS}} + \Delta_{\text{Link}}. \qquad [2]$$

[1] All uncertainties in this deliverable are reported with a coverage factor of k=1.
[2] Estimated uncertainty based on other more extensive BDOA calibration measurements.
[3] The Timing Switches contain the standard OHWR calibration values (firmware v5.0 / hardware v3.4) [8].

The asymmetry that is caused by the long-haul fiber link, Δ_{Link}, can therefore be calculated with

$$\Delta_{\mathrm{Link}} = \Delta - (\Delta_{\mathrm{TF\,GM}} + \Delta_{\mathrm{TF\,Slave}} + \Delta_{\mathrm{BDOA}} + \Delta_{\mathrm{TS}}). \qquad [3]$$

The measurement of Δ resulted in a total asymmetry of (-888 $\pm$ 20) ps. Δ_{Link} can now be calculated using all delay asymmetries listed in Table 5.2, together with Equation [3]. Using this method, a link asymmetry of (544 $\pm$ 39) ps is found.

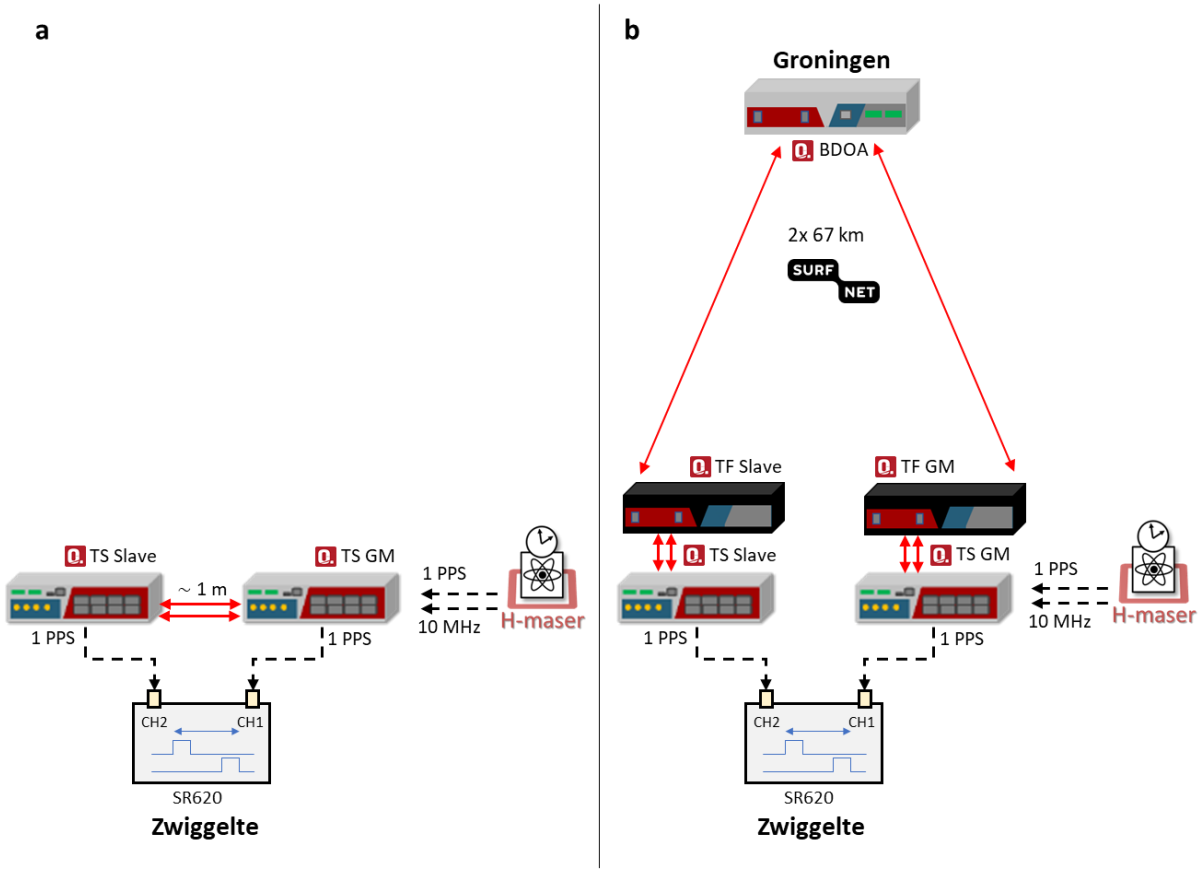

Figure 5.6: (a) Setup used for a reference measurement of the 1 PPS phase difference between the TS GM and TS Slave. (b) Setup used for a measurement of the 1 PPS phase difference between the TS GM and TS Slave including 2x67 km of optical fiber, Timing Filters and one BDOA.

Note that the link asymmetry must be treated different from a device delay asymmetry. The device delay asymmetry originates from the temporal delay differences caused by fiber length differences between the upstream and downstream paths within the device. The link asymmetry, however, does not originate from fiber length differences. Moreover, the up- and downstream signals travel through the same optical fiber. This delay asymmetry is in fact proportional to the total optical fiber length and the CD parameter of the optical fiber. If the

optical fiber length would change, the link asymmetry would also change. Therefore, the link asymmetry is not treated as an absolute temporal delay but as a factor, α, that is proportional to the round-trip time delay (RTT) through the long-haul fiber link:

$$\alpha = \frac{2\Delta_{\mathrm{Link}}}{\frac{1}{2}RTT - \Delta_{\mathrm{Link}}}. \qquad [4]$$

When α is incorporated in the Timing Switches, the WR protocol uses α to calculate and correct for the real-time link asymmetry by using real-time measurements of RTT. Filling in Δ_{Link} and the simultaneously measured RTT results in an α value of $(1.7 \pm 0.2) \times 10^{-6}$.

A major contribution to the measured uncertainty is that upon link restart, output PPS timing of the WR device will randomly shift with a standard deviation of $\sim$ 25ps [6]. This affects the accuracy with which one can determine the timing shift that is caused by the CD, and its contribution is listed as 'Restart' in Table 5.2. Another source of error listed in Table 5.2 is the difference in received optical power levels between the 'short' link (with attenuators) and the full-length path. The delay of the optical receiver in the SFP is somewhat dependent on the received input power.

Table 5.2: Overview of all delay asymmetry results

	Asymmetry (ps)	Uncertainty (ps) (k=1)
Δ	888	20
$\Delta_{\mathrm{TF\ GM}}$	-38	12
$\Delta_{\mathrm{TF\ Slave}}$	-53	11
Δ_{BDOA}	791	20
Δ_{TS}	-356	20
Power	0	10
Restart	0	25
Δ_{Link}	**544**	**47**

The link asymmetry is not only measured but also estimated using the CD specifications of the fiber links between Zwiggelte and Groningen. Table 5.3 lists the specifications for the two fiber links, with a resulting estimated link asymmetry, $\widetilde{\Delta}_{\mathrm{Link}}$ of 635 ps. This calculation has its own uncertainties such as the uncertainty of the fiber path length and dispersion values. The major contribution however is in the uncertainty of the SFP laser wavelength, which according to the manufacturer specifications is about 0.1nm. The dispersion calculation is

$$\Delta t = \frac{\Delta\lambda}{D \times L/2} \qquad [5]$$

where $\Delta\lambda$ is the wavelength difference between the two counter-propagating optical signals, D is the CD of the fiber and L is the length of the fiber. Given the wavelength specification, we

assume that the uncertainty of the wavelength difference is 0.14 nm. On an actual difference of 0.76 nm, this amounts to 18%. The length and dispersion measurements themselves also contribute to the uncertainty, but at a much lower level.

Table 5.3: Specifications of the optical fiber links between Zwiggelte (ZWT001A) and Groningen (GN012A) delivered by SURFnet.

Parameter	ZWT001A → GN012A	GN012A → ZWT001A
Length (km)	66.834	66.810
D(ps/nm/km)@1511	12.51	12.46
D(ps/nm/km)@1512	12.57	12.52
$\widetilde{\Delta}_{\mathrm{Link,x}}$ (ps)	**318**	**317**
$\widetilde{\Delta}_{\mathrm{Link}}$ (ps)	**635 ± 117**	

Predicting the link asymmetry from measured length and dispersion values is less accurate than actually measuring it, but provides a good sanity check. The measured and predicted values are in good agreement, within the estimated uncertainties. The offset and its uncertainty are all below 1 ns, and well below the 15 µs requirement.

6 Conclusions

Infrastructure in support of a bi-directional amplified connection between a White Rabbit master and slave switch has been deployed. Over this infrastructure SURFnet operates a bi-directional alien wave between these two switches. Although the fiber infrastructure has significantly changed this did not impact the performance and the ability to deploy this service. This is also the first time SURFnet has used a special filter dedicated to support niche photonic services in co-existence with carrier services for its services.

During the process of architecture, design, deployment and operation, lessons learnt have been identified and best practices have been recorded to be applied for future services in different parts of the network and for different photonic services.

The TFT performance measurements show that the frequency stability of the 134 km TFT link is already within two times the frequency stability of a brand-new hydrogen maser after 1000 s of averaging, and within one order of magnitude for all averaging times. Further research would need to identify the cause of the observed long-term phase difference variations. As mentioned one of the possible causes is the wavelength variation of the optical transmitters. Other effects like polarization mode dispersion should also be included in further research [7].

The link asymmetry caused by CD results in a measured phase difference of (544 ± 47) ps. The measured phase difference and the estimated phase difference (using the optical fiber characteristics) are in good agreement with each other. However, measuring the phase difference gives a more accurate result.

6.1 Future Work

The closing deliverable of the Cleopatra work-package is D5.14, where we will demonstrate actual VLBI observations using the transported timing signal. These VLBI observations will be used to perform an independent characterization of the timing link performance. Current activities include closing the remaining fiber gap of 300 m to the CAMRAS telescope, and then extending the link calibration to cover the complete link length. In the same deliverable, we will also bring the timing signal to the LOFAR concentrator node in Buinen.

This deliverable describes the first setup of the service where SURFnet will work with involved parties to optimize and adjust the TFT service to reach end-user satisfaction. Once this has been completed the service will be brought under monitoring of the NOC and work instructions for NOC and field engineers will be created. Together with the architecture and design rules outlined in D5.1, future (beyond the ASTERICS Project) TFT services will be rolled out on a case-by-case basis on SURFnet's new fiber plant and photonic transport infrastructure.

7 References

[1] "OHWR," [Online]. Available: https://www.ohwr.org/projects/white-rabbit/wiki.

[2] C. van Tour and J. Koelemeij, "ngVLA Memo #22," [Online]. Available: http://library.nrao.edu/public/memos/ngvla/NGVLA_22.pdf.

[3] B. Alachkar, A. Wilkinson and K. Grainge, "Frequency Reference Stability and Coherence Loss in Radio Astronomy Interferometers Application to the SKA," *Journal of Astronomical Instrumentation,* vol. 07, no. 01, 2018.

[4] M. Rizzi, "OHWR - wrs-low-jitter," [Online]. Available: https://www.ohwr.org/projects/wrs-low-jitter/wiki.

[5] H. Li, G. Gong, W. Pan, Q. Du and J. Li, "Temperature Effect on White Rabbit Timing Link," *IEEE Trans. Nucl . Sci.,* vol. 62, no. 3, pp. 1021-1026, 2015.

[6] P. Boven, "DWDM Stabilized Optics for White Rabbit," *IEEE,* vol. 2018 European Frequency and Time Forum (EFTF), 2018.

[7] P. A. Williams, W. C. Swann and N. R. Newbury, "High-stability transfer of an optical frequency over long fiber-optic links," *J. Opt. Soc. Am. B,* vol. 25, no. 8, 2008.

[8] "OHWR white-rabbit wiki calibration," [Online]. Available: https://www.ohwr.org/projects/white-rabbit/wiki/Calibration.

Appendix

Table 0.1 List of equipment used during measurements described in this deliverable.

Abbreviation	Description	Part Number	Serial Number
WR GM	OPNT Timing Switch	TS-18-21	TS2017000012
WR Slave	OPNT Timing Switch	TS-18-11	TS2017000019
TF GM	OPNT Timing Filter	TF-O-1-A-LP-02	TF2018000020
TF Slave	OPNT Timing Filter	TF-O-1-B-LP-02	TF2018000022
BDOA	OPNT Timing Amplifier	TA-SOA-O-LP-01	TA2017000011
TIC	Stanford Research Systems Time Interval Counter	SR620	0831
Phase noise test probe	Microsemi 3120A Phase noise test probe	3120A	SCA161800D8F

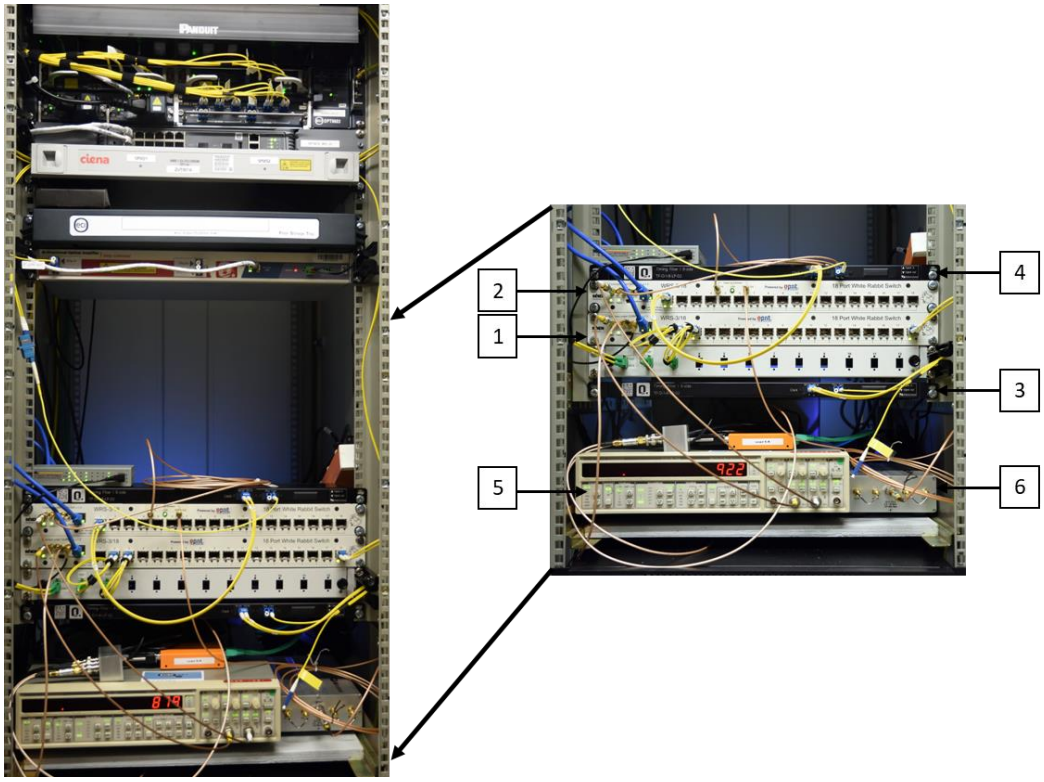

Figure 0.1 Setup in Zwiggelte with on the left: on top the SURFnet equipment and on the bottom the TFT equipment. Right: Zoom-in of the TFT equipment: [1] TS GM, [2] TS Slave, [3] TF GM, [4] TF Slave, [5] TIC Measurement device, [6] Microsemi 3120A phase noise test probe

Figure 0.2 The H-maser at the WRST location in Zwiggelte (covers removed due to maintenance).